

# Design of novel double-layer wrapped ammonium polyphosphate and its application in aging-resistant and flame retardant crosslinked polyethylene composites

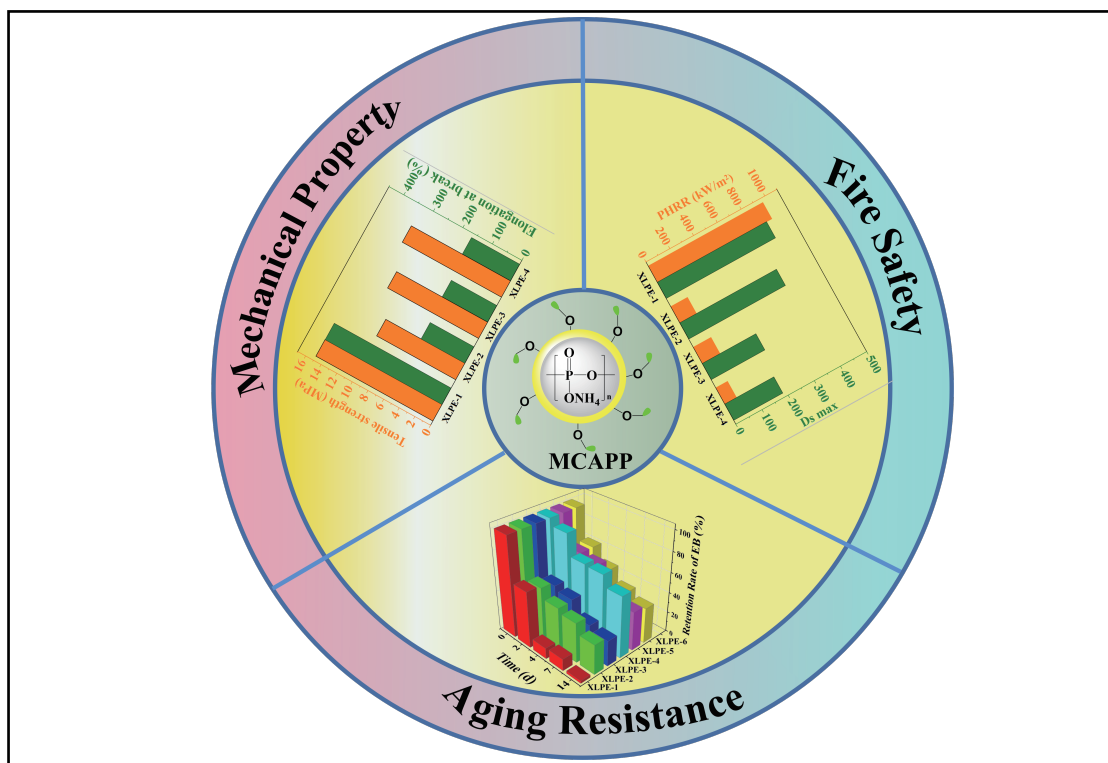
Pengfei Jia, Pengfei Sun, Fuhao Yu, Lei Song, Yuan Hu , and Bibo Wang 

State Key Laboratory of Fire Science, University of Science and Technology of China, Hefei 230027, China

 Correspondence: Yuan Hu, E-mail: [yuanhu@ustc.edu.cn](mailto:yuanhu@ustc.edu.cn); Bibo Wang, E-mail: [wbibo@ustc.edu.cn](mailto:wbibo@ustc.edu.cn)

© 2023 The Author(s). This is an open access article under the CC BY-NC-ND 4.0 license (<http://creativecommons.org/licenses/by-nc-nd/4.0/>).

## Graphical abstract





The double-layer wrapped ammonium polyphosphate (APP) enhances the fire safety, aging resistance, and mechanical property of crosslinked polyethylene (XLPE) composites.

## Public summary

- The double-layer wrapped ammonium polyphosphate (APP) enhances the compatibility and mechanical property of crosslinked polyethylene (XLPE) composites.
- The OIT value of XLPE-4 composite is 182.95 min, which is approximately 8 times than that of XLPE-1.
- After aging at 135 °C for 14 d, the retention of EB for XLPE-1 and XLPE-4 reaches 2.6% and 61.1%, respectively.
- The PHRR and Ds-max of XLPE-4 are reduced by 89.7% and 54.9%, respectively.

# Design of novel double-layer wrapped ammonium polyphosphate and its application in aging-resistant and flame retardant crosslinked polyethylene composites

Pengfei Jia, Pengfei Sun, Fuhao Yu, Lei Song, Yuan Hu , and Bibo Wang 

State Key Laboratory of Fire Science, University of Science and Technology of China, Hefei 230027, China

 Correspondence: Yuan Hu, E-mail: [yuanhu@ustc.edu.cn](mailto:yuanhu@ustc.edu.cn); Bibo Wang, E-mail: [wbibo@ustc.edu.cn](mailto:wbibo@ustc.edu.cn)

© 2023 The Author(s). This is an open access article under the CC BY-NC-ND 4.0 license (<http://creativecommons.org/licenses/by-nc-nd/4.0/>).



Cite This: *JUSTC*, 2023, 53(10): 1003 (9pp)



Read Online



Supporting Information

**Abstract:** In this study, double-layer wrapped ammonium polyphosphate (APP) is designed to enhance the mechanical properties, resistance and flame retardancy of crosslinked polyethylene (XLPE) composites. APP was wrapped with silica and then grafted with hindered phenol antioxidant 3-(3,5-di-tert-butyl-4 hydroxyphenyl) (AO) to prepare double-layer wrapped flame retardants (MCAPP). Due to the excellent compatibility between the MCAPP and XLPE matrix, the tensile strength and elongation at break of XLPE/MCAPP/CFA (XLPE-4) were improved. Moreover, the retention rate of elongation at break for the XLPE-4 composite reached 61.1%, significantly higher than that of XLPE-1 (2.6%) at 135 °C after aging for 14 d. This demonstrates that MCAPP could improve the aging resistance of XLPE cable composites. Compared with XLPE-1, the maximum smoke density and the peak heat release rate were reduced by 54.9% and 89.7%, respectively. Thus, the double-layer wrapping antioxidant strategy provides an excellent approach to obtain high-performance XLPE composites.

**Keywords:** wrapped ammonium polyphosphate; XLPE cable; aging resistance; fire safety; mechanical property

**CLC number:** TM249.5

**Document code:** A

## 1 Introduction

Polyethylene (PE) has the advantages of low density, good toughness, high elongation, easy processing, and low cost, and is widely used in industrial packaging, building, transportation, electrical and electronics fields<sup>[1-3]</sup>. However, PE has a lower limiting oxygen index (LOI) and higher flammability, hindering its application in some fields. The flame retardancy of the PE matrix can be effectively improved by doping with flame retardants. Traditional halogenated flame retardants have good flame retardancy, but they release toxic gas and corrosive smoke to pollute the environment. Inorganic flame retardants, such as magnesium hydroxide and aluminum hydroxide, have the advantages of low cost and non-toxicity<sup>[4-6]</sup>. However, the addition amount of magnesium hydroxide or aluminum hydroxide is usually higher, resulting in a decrease in the mechanical properties of the composite materials<sup>[7-9]</sup>.

In recent years, intumescent flame retardants (IFRs) based on ammonium polyphosphate (APP) have shown good flame resistance, non-toxicity, and low smoke<sup>[10-12]</sup>. Liu et al.<sup>[13]</sup> doped 30% IFR (SPEPO : APP : MP = 7 : 7 : 1) in LDPE, and the LOI of the composite was 27.6%, reaching the V-0 level for UL-94. However, IFRs have some shortcomings in flame retarding polymers, such as poor compatibility with polymers and strong hygroscopicity. The mechanical properties and durability of IFR flame retardant materials are greatly reduced. APP particularly easily absorbs moisture, resulting

in poor water resistance of the polymer. Microencapsulation of APP and macromolecular carbon-forming agents (CFAs) can effectively improve these defects to improve the compatibility and durability of flame retardant polymer composites<sup>[14-16]</sup>.

In general, PE is also easily subjected to thermal oxidation and degradation during the long-term service process, resulting in an overall decrease in the mechanical, electrical, and service performances of PE composites. The most common and valid way to enhance the aging resistance of PE composites is adding antioxidants to the PE matrix. The antioxidant can capture free radicals produced from the degradation of the PE composites to stabilize the matrix. Nevertheless, commonly used antioxidants have relatively small molecular weights, poor thermal stability, easy volatilization, migration resistance, and other defects in the process of usage, so the actual application efficiency of antioxidants is reduced<sup>[17-19]</sup>. To solve these above problems, the current research mainly focuses on loaded antioxidants and polymer antioxidants, increasing the molecular weight of the antioxidant, passing physical adsorption or chemical reaction to graft low molecular weight antioxidants on the inorganic filler<sup>[20]</sup>. Li et al.<sup>[21]</sup> took titanium dioxide coated with silica as the carrier (SiO<sub>2</sub>-TiO<sub>2</sub>), used 3-aminopropyl triethoxysilane (KH550) for modification and then grafted AO onto the carrier to obtain the supporting antioxidant (AO-KH550-SiO<sub>2</sub>-TiO<sub>2</sub>). When AO-KH550-SiO<sub>2</sub>-TiO<sub>2</sub> is added to polypropylene (PP) directly, its

oxidation induction time (OIT) value is the highest, and the carbonyl index does not surge after aging, indicating that the embedded antioxidant has good thermal oxygen stability<sup>[22]</sup>.

The hindered phenol antioxidant 3-(3,5-ditert-butyl-4-hydroxyphenyl) propionate (AO) can capture RO and ROO radicals to inhibit the aging process of polymer materials and is widely used as a primary antioxidant in polymer materials. Upon mixing with AO, APP may affect the efficiency of AO<sup>[23]</sup>. In addition, the small molecule antioxidant, AO, easily suffers from physical losses, e.g., volatilization, migration, and water extraction, which need to be fixed on other solid surfaces<sup>[24]</sup>. Combining AO with APP seems to be an attractive way to confer inherent properties to both components through design and control. The silane coupling agent is an organic silicon that can improve the water resistance of APP and the interface compatibility between APP and the polymer matrix<sup>[25]</sup>. It is made from the hydrolysis of siloxane in water. The above issues can be solved by wrapping APP with a layer of silicone and AO simultaneously.

Herein, to further improve the compatibility and long-term aging resistance of APP-based IFRs and expand their application field, APP-based IFRs were treated with an organosilane coupling agent and AO to modify the surface. The effects of double-layer APP-based IFRs on the flame retardant, mechanical properties and aging resistance of XLPE cable were studied by using thermogravimetric analysis (TGA), the LOI, UL-94, conical calorimeter (Cone), smoke density, differential scanning calorimetry (DSC) test, and physical properties tests.

## 2 Experimental part

### 2.1 Preparation of AO-Cl

The synthesis of 3,5-ditert-butyl-4-hydroxyphenylpre-nonyl chloride (AO-Cl) can be seen in the Supporting information.

### 2.2 Preparation of MCAPP

**Step 1:** The synthesis of SiAPP can be seen in Ref. [26].

**Step 2:** SiAPP (100 g), triethylamine (2.1 g) and trichloromethane (200 mL) were added to a 500 mL three-neck flask and stirred constantly at 45 °C. After that, 5.7 g of AO-Cl was dripped into the above solution and reacted for 4 h at 45 °C. After that, the mixture was placed at 25 °C, filtered and washed with water and trichloromethane. Then, these products were dried at 80 °C for 9 h (Fig. 1a) to obtain the MCAPP.

### 2.3 Fabrication of XLPE composites

MCAPP (16.5 wt%), 5.5 wt% CFA, and 78 wt% PE were added to an internal mixer, which was melted at 110 °C at a speed of 40 r/min. Then, 0.6% triallyl cyanate (TAIC) and 0.6% diisopropylene benzene peroxide (DCP) were poured into the above mixture for mixing evenly. After that, these XLPE mixtures were hot pressed at 160 °C for 15 min, and the standard size and shape were prepared for testing (XLPE-4). In a further attempt to compare the performance of the MCAPP and the mixture of APP and AO, the comparative formula is shown in Table 1 to compare the comprehensive properties of these samples.

## 3 Results and discussion

### 3.1 The characterization of MCAPP

As shown in Fig. 1b, the hydrophilicity on the surface of the flame retardants was investigated using a contact angle meter. The contact angle of APP is 29.1°, indicating that APP is very hydrophilic. After wrapping SiO<sub>2</sub> on the APP surface, the contact angle of SiAPP was 15.3°, because hydrophilic Si-OH was introduced into the shell surrounding the SiAPP, thus improving the hydrophilicity of the flame retardant. The contact angle of MCAPP is 91.7°, indicating that the surface of the flame retardant becomes more hydrophobic after wrapping with aromatic AO. Therefore, the problem of poor water resistance and poor compatibility with the PE matrix could be solved. Moreover, it can be seen from Fig. 1c that the APP presents a stacked irregular particle-like structure, and the surface gradually becomes rougher after SiO<sub>2</sub> and hindered phenol wrapping. In addition, SEM mapping was also performed on the surface elements of MCAPP in Fig. 1d. The simultaneous detection of C, O, Si, and P elements in Fig. 1d indicated that the MCAPP was successfully prepared.

Fig. 2a shows the Fourier transform infrared (FTIR) spectra of APP, SiAPP, and MCAPP. Obviously, the absorption peak at 3485 cm<sup>-1</sup> is attributed to the stretching vibration of -OH. The bending vibration peaks at 980 cm<sup>-1</sup> and the stretching vibration peak at 885 cm<sup>-1</sup> are attributed to the P-OH bond and P-O-P bond of APP, respectively. After APP is microencapsulated with silica (SiAPP), 1110 cm<sup>-1</sup> corresponds to asymmetric Si-O-Si bonds. After grafting AO to SiAPP, a new absorption peak appeared at 1750 cm<sup>-1</sup>, which corresponds to the C=O of AO<sup>[27]</sup>. These results demonstrate that AO is successfully grafted onto the surface of SiAPP. Fig. 2b and Fig. S1 show the chemical composition of APP, SiAPP, and MCAPP by X-ray photoelectron spectroscopy (XPS) spectra. Compared with APP, the content of C and Si on the surface of SiAPP increased, which indicates that SiO<sub>2</sub> was successfully hydrolyzed on the surface of APP. Meanwhile, the content of C element on the surface of MCAPP increases, while the content of Si element decreases, demonstrating successful grafting from SiAPP with AO.

The TGA curves and relevant data obtained for the studied samples APP, SiAPP, and MCAPP are shown in Fig. 2c and Table S1.  $T_{-5\text{wt}\%}$ ,  $T_{-10\text{wt}\%}$ , and  $T_{\text{max}}$  are the temperatures where the weight loss is 5 wt%, 10 wt%, and the weight-loss rate reaches its maximum, respectively. The char residue of APP at 800 °C is 11.1 wt%, which indicates the good thermal stability and carbonization ability of the flame retardant. The char residues of SiAPP and MCAPP at 800 °C are 44.7 wt% and 38.0 wt%, respectively, both of which are higher than that of APP. The relative grafting ratio of AO on SiAPP was calculated to be approximately 16.3 wt%, and the relevant calculation process can be seen in Table S2.

Fig. 2d shows the different radical scavenging activities of APP, SiAPP, MCAPP, and AO toward 2,2-Diphenyl-1-picrylhydrazyl (DPPH) free radicals<sup>[28]</sup>. The radical scavenging activity of the stabilizer increased with increasing

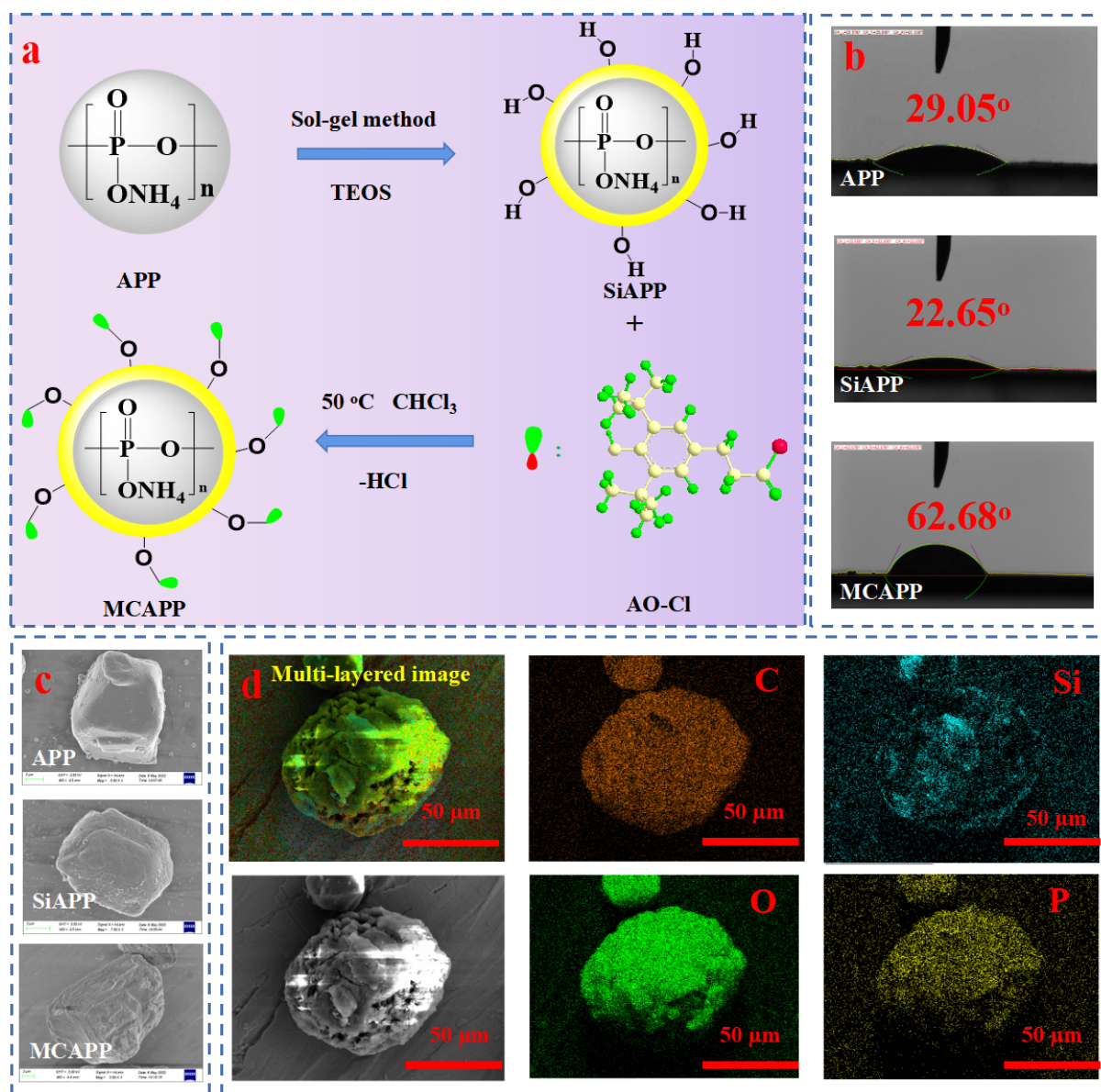


**Fig. 1.** (a) Schematic representation of the preparation process of MCAPP. (b) The corresponding WCA optical images. (c) SEM images of APP, SiAPP, and MCAPP. (d) EDX mapping images of MCAPP.

**Table 1.** Formulas of the XLPE composites.

Sample	PE	APP	SiAPP	CFA	MCAPP	AO	TAIC	DCP	UL-94	LOI
XLPE-1	100						1.5	0.6	NR	17%
XLPE-2	78	16.5		5.5			0.6	0.6	V2	24%
XLPE-3	78		16.5	5.5			0.6	0.6	V0	27%
XLPE-4	78			5.5	16.5		0.6	0.6	V0	29%
XLPE-5	78	15.34		5.11		1.55	0.6	0.6	V2	26%
XLPE-6	78		15.34	5.11		1.55	0.6	0.6	V0	28%

sample concentration, as shown in Fig. 2d. The scavenging activity of APP and SiAPP was basically maintained at very low levels with increasing concentration, which was much lower than that of MCAPP. In addition, with increasing stabilizer concentration, the free radical scavenging activity of MCAPP approaches that of AO, indicating that grafting with

AO enhances the free radical scavenging ability of MCAPP, which may effectively delay the degradation of XLPE.

### 3.2 Mechanical property and dispersion analysis

One of the most critical properties of polymer materials is their mechanical properties<sup>[29]</sup>. The mechanical properties of

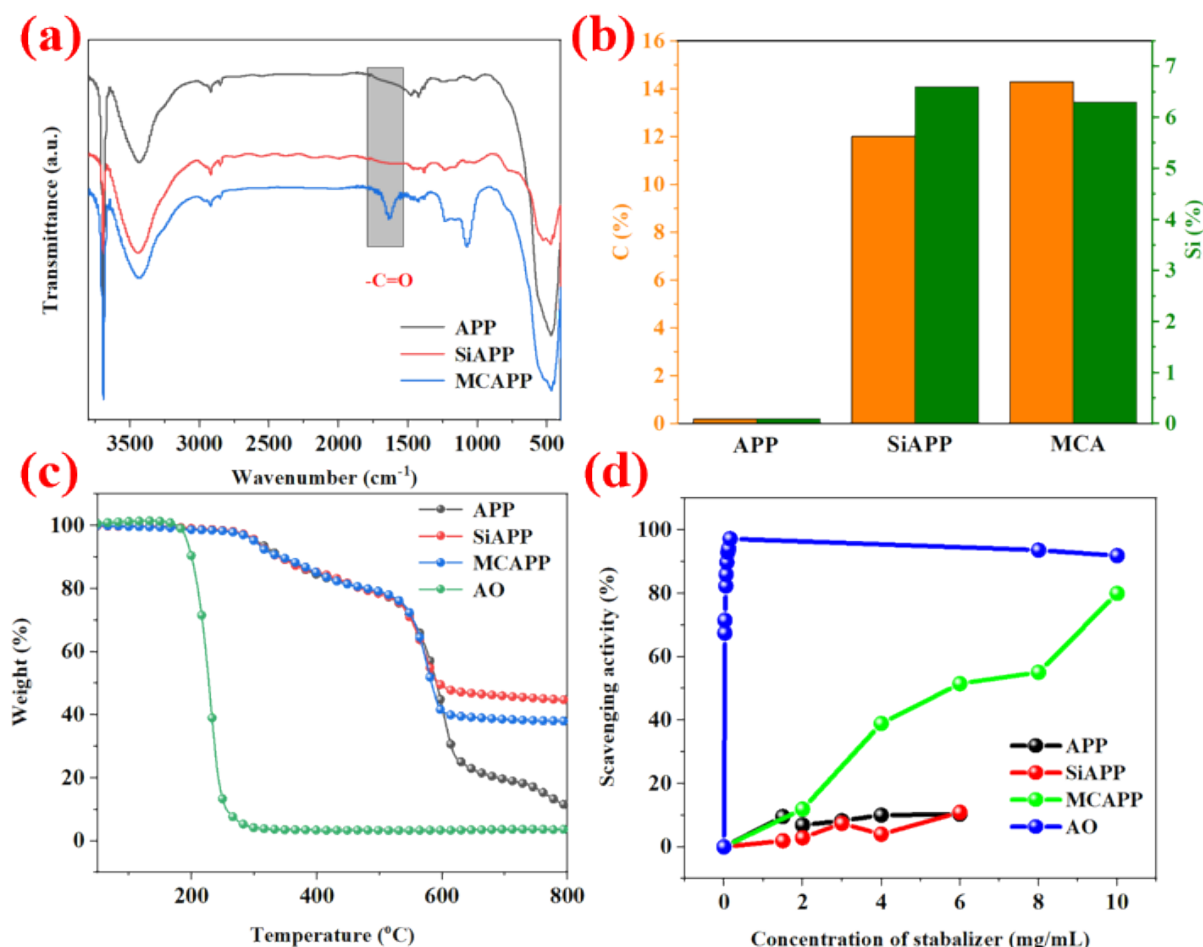


**Fig. 2.** (a) FTIR spectra of APP, SiAPP, and MCAPP. (b) The contents of C 1s and Si 2p from APP, SiAPP, and MCAPP. (c) TGA curves of APP, SiAPP, MCAPP, and AO under N<sub>2</sub> atmosphere. (d) Radical scavenging activity of APP, SiAPP, MCAPP, and AO.

XLPE and its composites were investigated using a universal testing machine. Fig. 3a and b shows that the tensile strength (TS) and elongation at break (EB) of XLPE-1 reach 15.0 MPa and 396%, respectively. When APP was added to XLPE, the TS and EB of XLPE-2 were reduced to 10.1 MPa and 149%, respectively. For XLPE-3, the TS and EB are 11.8 MPa and 154%, respectively. These results indicate that the mechanical properties of XLPE composites deteriorate sharply by increasing the loading of APP and SiAPP. At the same time, the introduction of AO slightly enhances the mechanical properties of XLPE-5 and XLPE-6. However, for XLPE-4, the TS and EB increase to 12.7 MPa and 163%, respectively. These above results indicate that organic benzene rings improve the compatibility of polar flame retardants, thus improving the mechanical properties.

To further explore the distribution status of MCAPP, the cross-sectional morphologies of XLPE composites are shown in Fig. 3c–j. There are many obvious interfaces between APP (or SiAPP) and the XLPE matrix. The interface between these flame retardants and the XLPE matrix is poor, as proven by the obvious holes and interfaces in the XLPE-1 and XLPE-2 sections. However, MCAPP is evenly distributed in the XLPE matrix, and there is no obvious incompatible interface and hole distribution, indicating that MCAPP is compatible with the XLPE matrix. The excellent and uniform dispersion and

interfacial adhesion of MCAPP greatly affect the mechanical properties of XLPE composites.

### 3.3 Aging resistance performance

In the DSC test, oxidation induction time (OIT) is considered an important indicator of antioxidant performance<sup>[30–31]</sup>. In general, the longer the OIT value, the better the sample antioxidant degradation performance. Fig. 4a and b shows the OIT values of these XLPE composites. The OIT values of the XLPE-1, XLPE-2, and XLPE-3 composites were 24.0 min, 19.16 min, and 38.19 min before extraction, indicating that thermal oxidation occurs rapidly under oxygen. The OIT values of XLPE-4, XLPE-5, and XLPE-6 increased significantly to 182.95 min, 53.47 min, and 68.13 min, respectively, showing that the introduction of AO improved the aging resistance of the XLPE composites.

In practical applications, XLPE composites are commonly applied in an air atmosphere. To study the antioxidant capacity of MCAPP, an accelerated thermal oxidative aging test was performed. Moreover, the relationship between the EB of the XLPE composites with different antioxidants and the change rate of the 135 °C aging time is shown in Fig. 4c. The XLPE-1, XLPE-2, and XLPE-3 composites showed significant deterioration after aging for 14 d, and the retention of EB reached 2.6%, 29.8%, and 25.5%, respectively, without aging-

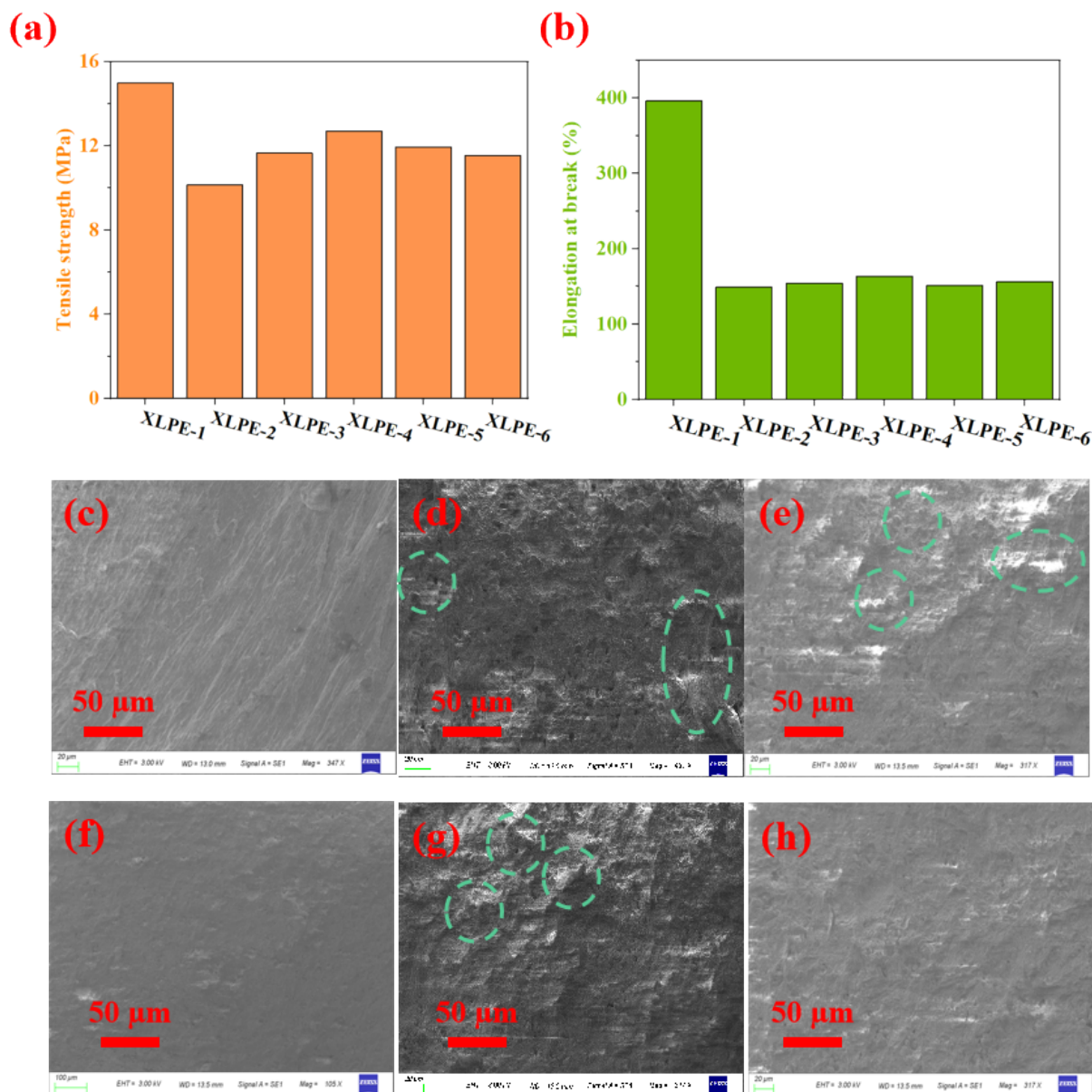


**Fig. 3.** (a) Tensile strength, (b) elongation at break and (c–j) cross-sectional SEM images of XLPE-1, XLPE-2, XLPE-3, XLPE-4, XLPE-5, and XLPE-6.

resistant AO components. Meanwhile, the retention of EB from the XLEVA-5 and XLEVA-6 composites was 38.8% and 35.2%, respectively. For the XLEVA-4 composite, the retention of EB reached 61.1% after aging, showing excellent aging resistance. This is because the small molecule AO more easily migrates to the surface and volatilizes than the AO grafted to the MCAPP surface, which affects its long-term aging resistance. Therefore, for long-term practical applications, MCAPP is an effective anti-aging agent for XLPE composites.

To study the aging resistance mechanism of XLPE composites<sup>[32]</sup>, electron spin spectroscopy (ESR) was used to test the concentration of single-electron radicals before and after aging at 135 °C for 14 d (Fig. 4c and d). The complex containing AO has a low radical concentration, and XLPE-4 has the lowest radical concentration after aging, indicating that the AO components play a role in free radical scavenging to

endow these XLPE composites with aging resistance. The above results are consistent with the mechanical property changes of XLPE composites after aging, further demonstrating that MCAPP has an effect on the long-term aging process of XLPE.

### 3.4 Fire safety

The TGA and DTG curves of these XLPE composites under N<sub>2</sub> and the corresponding data are recorded in Fig. 5a, b, and Table S4. As shown in Fig. 5a, the flame-retardant XLPE composites have higher initial decomposition temperatures than pure XLPE. At the same time, compared with pure XLPE, flame retardant XLPE samples have better thermal stability and more char residue in the temperature interval of 400–750 °C. This is because flame retardants at high temperature produce a dense char layer, which can act as a barrier to protect the matrix. Compared with the XLPE-2 and XLPE-3

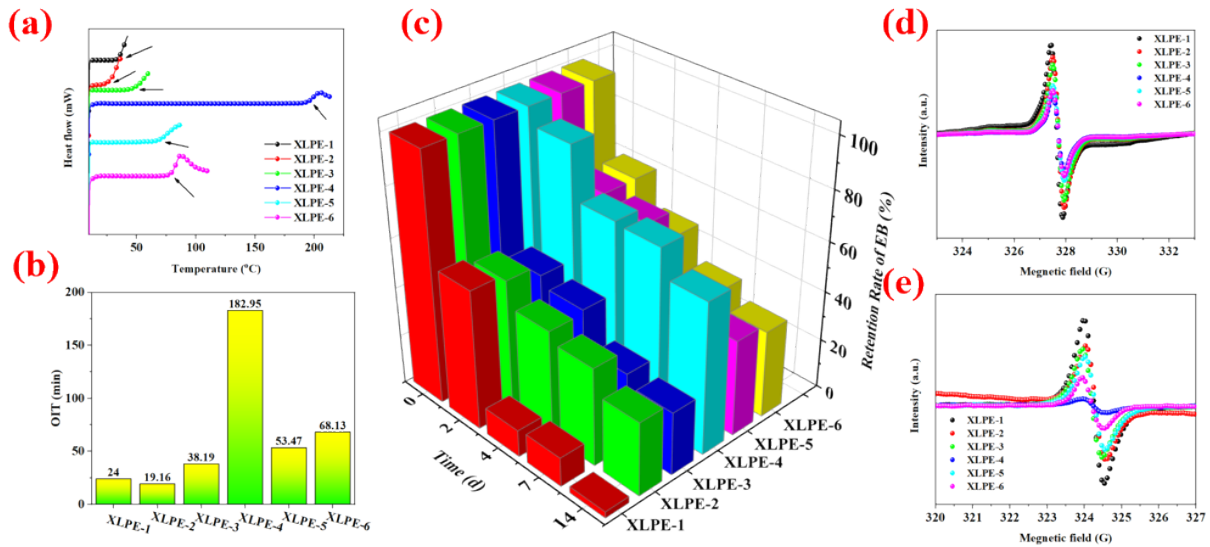


**Fig. 4.** (a, b) The OIT curves of XLPE composites at 210 °C. (c) Retention rate of elongation at break of XLPE composites with different aging times at 135 °C. Electron spin resonance spectra of XLPE composites before (d) and after (e) aging at 135 °C for 14 d.

systems, XLPE-4 has lower initial decomposition temperatures and maximum mass loss but has higher thermal stability and higher char production. This is attributed to the silicon shell participating in char formation to enhance the stability of the char layer and efficiently protect the XLPE matrix in the high-temperature stage<sup>[33]</sup>.

These LOI values and UL-94 ratings of the XLPE composites are recorded in Table 2. When APP is added, the LOI of the XLPE composites increases from 17% to 24%, and the UL-94 rating of the XLPE composites increases from no rating (NR) to V2. At the same loading, XLPE-4 had the highest LOI value of 29%, and the UL-94 rating could pass V0. The above results show that XLPE-4 exhibits excellent flame retardancy.

It can be seen from Fig. 5c, d, and Table 2 that a cone calorimeter is used to study the combustion performance of flame retardant XLPE composites<sup>[34]</sup>. Various data, including the fire growth index (FGI), fire performance index (FPI), time to ignition (TTI), peak heat release rate (pHRR), time to peak heat release rate ( $T_{pHRR}$ ), and total heat release (THR), are recorded in Table 2. XLPE-1 reaches a pHRR of 965 kW/m<sup>2</sup> at 156 s and then burns completely at 350 s, indicating that pure XLPE burns very easily. After the addition of flame retardants, the pHRR of the XLPE composites is significantly reduced. The pHRR of XLPE-4 is only 99 kW/m<sup>2</sup>, which is 89.7% lower than that of XLPE-1. Moreover, the pHRR of XLPE-2 is 141 kW/m<sup>2</sup>, which is higher than that of MCAPP.

At the same time, the THR curve shows a similar trend, and the THR of XLPE-4 is only 58.39 kW/m<sup>2</sup>, which is 33.4% lower than that of XLPE-1. To further evaluate the fire hazard of XLPE composites, their FPI was calculated. The FPI is obtained according to the ratio of TTI to pHRR. The FPI value decreases, which indicates that the fire risk of XLPE composites is increased. The FPI value of XLPE-4 is higher than that of XLPE-1, showing that it has higher fire safety. The above result demonstrates that the double-layer wrapped APP can significantly enhance the fire safety of XLPE composites.

In general, the toxic smoke produced from burning in fires is the main cause of casualties<sup>[35]</sup>. Thus, it is crucial to evaluate the impact of MCAPP on the nonthermal hazard of PE. The maximum smoke density ( $D_s\text{-max}$ ) value and smoke transmittance curve are shown in Fig. 5e and f. The  $D_s\text{-max}$  of XLPE composites with flame retardants is significantly reduced. Compared with that of XLPE-1, the  $D_s\text{-max}$  of XLPE-4 is only 188.4 m<sup>2</sup>/m<sup>2</sup>, which is reduced by 54.9%. Due to the excellent carbonization properties of the XLPE-4 composites, the dense carbon layer has a good physical barrier effect. It could delay the escape of volatile flue gas as well as flammable products produced from the degradation of the matrix and then delay the smoke release rate in the combustion process and inhibit the release of toxic flue gases.

These gas pyrolysis products for XLPE composites could be studied by thermogravimetric-infrared spectroscopy

**Table 2.** UL-94, LOI, and key parameters acquired from cone calorimetry tests.

Samples	TTI (s)	$T_{pHRR}$ (s)	pHRR (kW/m <sup>2</sup> )	THR (MJ/m <sup>2</sup> )	FPI (s·m <sup>2</sup> /kW)	UL-94	LOI
XLPE-1	62	156	965	87.65	0.064	NR	17%
XLPE-2	33	59	141	66.51	0.234	V2	24%
XLPE-3	26	50	150	66.50	0.173	V0	27%
XLPE-4	50	165	99	58.39	0.505	V0	29%
XLPE-5	68	150	129	61.67	0.527	V2	26%
XLPE-6	64	129	131	63.74	0.489	V0	28%

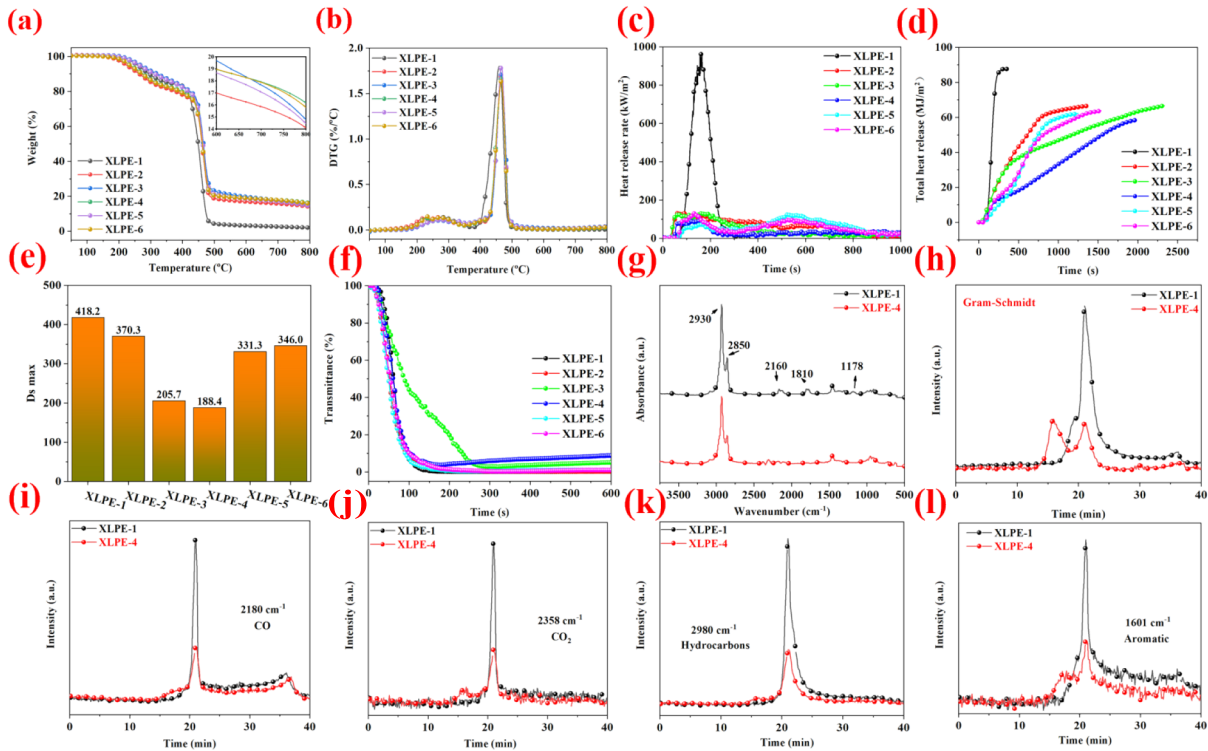


**Fig. 5.** (a, b) TGA and DTG curves for XLPE composites from 50 °C to 800 °C under a N<sub>2</sub> atmosphere, respectively. (c–f) HRR, THR curves, maximum smoke density, and smoke transmittance curve of XLPE composites respectively. (g, h) The absorbance at the maximum decomposition rate and Gram–Schmidt curves for XLPE-1 and XLPE-4. (i–l) Typical volatile thermal decomposition products versus time: CO, CO<sub>2</sub>, hydrocarbons, and aromatic.

(TG-IR). Fig. 5g and h present the absorbance at the maximum decomposition rate and Gram–Schmidt curves of XLPE composites<sup>[36]</sup>. Compared with the Gram–Schmidt curves and absorbance at the maximum decomposition rate temperature ( $T_{max}$ ) of XLPE-1, the peak release rates of the total pyrolysis products from XLPE-4 are significantly reduced, demonstrating that more components of XLPE-4 were reserved from the condensed phase. These absorption peaks at 2180 cm<sup>-1</sup>, 2358

cm<sup>-1</sup>, 2980 cm<sup>-1</sup>, and 1601 cm<sup>-1</sup> are attributed to the CO, CO<sub>2</sub>, hydrocarbons, and aromatic compounds of essential compounds produced in combustion (as shown in Fig. 5i–l). Notably, the combustible volatiles produced by XLPE-4 (hydrocarbons (2980 cm<sup>-1</sup>), aromatic compounds (1601 cm<sup>-1</sup>), and CO (2180 cm<sup>-1</sup>)) were much weaker than those produced by XLPE-1. Moreover, CO<sub>2</sub> is another important indicator of fire safety because a high concentration of CO<sub>2</sub> can easily

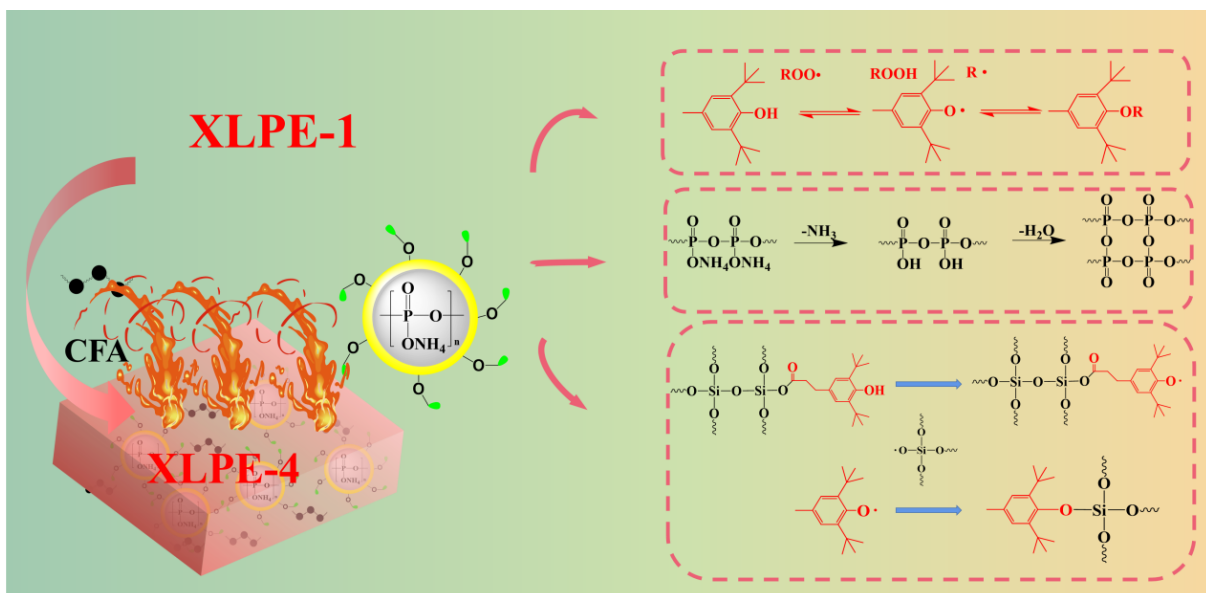


**Fig. 6.** Schematic diagram of the flame retardant mechanism of the XLPE-4 composite.



suffocate people in the event of fires<sup>[37–39]</sup>. The peak release rates of CO<sub>2</sub> from XLPE-4 are significantly reduced compared with those produced by XLPE-1, which is beneficial for inhibiting fire hazards. In summary, with the addition of MCAPP, the fuel supply and toxic gases are efficiently suppressed.

### 3.5 Flame retardant mechanism analysis

The synergistic flame retardant effect of MCAPP (see Fig. 6) was confirmed by the analysis of condensed and gas phases (Figs. S4, S5, and S6). The pure XLPE burns tempestuously under intense thermal radiation, releasing a large number of pyrolysis products, exhibiting severe fire hazards during burning. The addition of MCAPP could effectively improve the fire safety of XLPE composites. For the condensed phase, polyphosphate and biased phosphate produced by the decomposition of APP catalyze the degradation of the XLPE matrix, forming a coherent, partially graphitized, tight carbon layer by crosslinking reactions and esterification. Moreover, the release of NH<sub>3</sub> and H<sub>2</sub>O during APP decomposition not only has a gas phase dilution effect but also expands the carbonaceous layer. Thus, a constantly porous carbonaceous layer adheres on the substrate. The carbonaceous layer effectively inhibits oxygen and heat transfer to the combustion zone and prevents further degradation of the residual matrix. Meanwhile, the intumescent char layer restricts the escape of combustible gases to the flame zone, effectively preventing the extension of the fire. Finally, oxygen radicals generated from the AO in MCAPP can quench the alkyl and peroxide radicals, thereby preventing chain breakage and reducing smoke release. In addition, SiAPP is crosslinked with AO to form a compact char layer, and the SiO<sub>2</sub> generated from SiAPP decomposition strengthens the carbonaceous layer.

## 4 Conclusions

In this study, APP was wrapped with silica and then grafted with the hindered phenol antioxidant AO to prepare double-layer wrapped MCAPP, which was added to XLPE to enhance the service performance. The TS and EB of XLPE-4 were improved due to their excellent compatibility. Moreover, the introduction of AO on the surface of MCAPP can effectively capture free radicals during combustion and protect the XLPE matrix from thermal oxygen aging. After aging at 135 °C for 14 d, the retention rate of elongation at break increases by 61.1% for the XLPE-4 composite. Compared with XLPE-1, Ds-max, and pHRR were reduced by 54.9% and 89.7%, respectively. This work provides an effective method for preparing high-performance flame-retardant XLPE composites with excellent aging resistance.

## Supporting information

The supporting information for this article can be found online at <https://doi.org/10.52396/JUSTC-2023-0090>. The supporting information includes 4 tables and 6 figures.

## Acknowledgements

This work was supported by the Fundamental Research Funds

for the Central Universities (WK2320000054), National Natural Science Foundation of China (U1833113, 51874266) and the Experimental Center of Engineering and Material Science from University of Science and Technology of China.

## Conflict of interest

The authors declare that they have no conflict of interest.

## Biographies

**Pengfei Jia** is currently a postgraduate student in the State Key Laboratory of Fire Science, University of Science and Technology of China. His research mainly focuses on application about aging-resistant and flame-retardant crosslinked polyethylene composites.

**Yuan Hu** is an Professor and master supervisor at the State Key Laboratory of Fire Science, University of Science and Technology of China (USTC). He received his Ph.D. degree in Chemistry from USTC in 1997. His research mainly focuses on the New environmentally friendly flame retardant materials and technologies, high-performance polymer-based nanocomposites, as well as fire safety material research methods and technologies.

**Bibo Wang** is an Associate Professor and master supervisor at the State Key Laboratory of Fire Science, the University of Science and Technology of China. His research mainly focuses on the surface modification and microencapsulation technology of flame retardants, electron beam irradiation cross-linked flame retardant cables, aging performance, durability testing, and evaluation of flame retardant materials.

## References

- [1] Chen J, Wang J, Ding A, et al. Flame retardancy and mechanical properties of glass fibre reinforced polyethylene composites filled with novel intumescent flame retardant. *Composites Part B: Engineering*, **2019**, *179*: 107555.
- [2] Lau S, Gonchikzhapov M, Paletsky A, et al. Aluminum diethylphosphinate as a flame retardant for polyethylene: Investigation of the pyrolysis and combustion behavior of PE/AlPi-mixtures. *Combustion and Flame*, **2022**, *240*: 112006.
- [3] Salasinska K, Mizera K, Celiński M, et al. Thermal properties and fire behavior of polyethylene with a mixture of copper phosphate and melamine phosphate as a novel flame retardant. *Fire Safety Journal*, **2020**, *115*: 103137.
- [4] Wang C, Liu J, Wang Y, et al. Enhanced flame retardance in polyethylene/magnesium hydroxide/polycarbosilane blends. *Materials Chemistry and Physics*, **2020**, *253*: 123373.
- [5] Xie C, Leng F, Dong Z, et al. Synthesis of 9,10-dihydro-9-oxa-10-phosphaphenanthrene-10-oxide derivative grafted polyethylene films for improving the flame retardant and anti-dripping properties. *Polymer Engineering & Science*, **2020**, *60*: 2804–2813.
- [6] Yan J, Xu M. Design, synthesis and application of a highly efficient mono-component intumescent flame retardant for non-charring polyethylene composites. *Polymer Bulletin*, **2021**, *78*: 643–662.
- [7] Zhang T, Wang C, Wang Y, et al. Effects of modified layered double hydroxides on the thermal degradation and combustion behaviors of intumescent flame retardant polyethylene nanocomposites. *Polymers*, **2022**, *14*: 1616.
- [8] Birnbaum L S, Staskal D F. Brominated flame retardants: Cause for concern? *Environmental Health Perspectives*, **2004**, *112*: 9–17.
- [9] Rault F, Giraud S, Salaün F. Flame retardant/resistant based nanocomposites in textile. In: Visakh P, Arao Y, editors. *Flame Retardants*. Cham: Springer, 2015: 131–165.
- [10] Hu X P, Li Y L, Wang Y Z. Synergistic effect of the charring agent

- on the thermal and flame retardant properties of polyethylene. *Macromolecular Materials and Engineering*, **2004**, *289*: 208–212.
- [11] Li X, Yang B. Synergistic effects of pentaerythritol phosphate nickel salt (PPNS) with ammonium polyphosphate in flame retardant of polyethylene. *Journal of Thermal Analysis and Calorimetry*, **2015**, *122*: 359–368.
- [12] Barczewski M, Hejna A, Sałasińska K, et al. Thermomechanical and fire properties of polyethylene-composite-filled ammonium polyphosphate and inorganic fillers: An evaluation of their modification efficiency. *Polymers*, **2022**, *14*: 2501.
- [13] Liu Y, Wang D Y, Wang J S, et al. A novel intumescent flame-retardant LDPE system and its thermo-oxidative degradation and flame-retardant mechanisms. *Polymers for Advanced Technologies*, **2008**, *19*: 1566–1575.
- [14] Martín Z, Jiménez I, Gómez M Á, et al. Interfacial interactions in PP/MMT/SEBS nanocomposites. *Macromolecules*, **2010**, *43*: 448–453.
- [15] Ferdinánd M, Jerabek M, Várdai R, et al. Impact modification of wood flour reinforced PP composites: Problems, analysis, solution. *Composites Part A: Applied Science and Manufacturing*, **2023**, *167*: 107445.
- [16] Li Y, Chen X, Liu Q, et al. Constructing cross-functional intumescent flame retardants with UV resistance for polypropylene composites. *Materials Today Chemistry*, **2022**, *26*: 101048.
- [17] Xie H, Lai X, Li H, et al. Synthesis of a novel macromolecular charring agent with free-radical quenching capability and its synergism in flame retardant polypropylene. *Polymer Degradation and Stability*, **2016**, *130*: 68–77.
- [18] Zhang L, Li H, Lai X, et al. Functionalized graphene as an effective antioxidant in natural rubber. *Composites Part A: Applied Science and Manufacturing*, **2018**, *107*: 47–54.
- [19] Wang J, Zheng Y, Ren W, et al. Intrinsic ionic confinement dynamic engineering of ionomers with low dielectric-k, high healing and stretchability for electronic device reconfiguration. *Chemical Engineering Journal*, **2023**, *453*: 139837.
- [20] Zou Y, He J, Tang Z, et al. Structural and mechanical properties of styrene-butadiene rubber/silica composites with an interface modified in situ using a novel hindered phenol antioxidant and its samarium complex. *Composites Science and Technology*, **2020**, *188*: 107984.
- [21] Li G, Wang F, Liu P, et al. Antioxidant functionalized silica-coated TiO<sub>2</sub> nanorods to enhance the thermal and photo stability of polypropylene. *Applied Surface Science*, **2019**, *476*: 682–690.
- [22] Jiang S, Liu Y, Zou X, et al. Synthesis and application of new macromolecular hindered phenol antioxidants of polyamide 6. *Journal of Applied Polymer Science*, **2021**, *138*: 51184.
- [23] Li R, Shi K, Ye L, et al. Polyamide 6/graphene oxide-g-hindered phenol antioxidant nano-composites: Intercalation structure and synergistic thermal oxidative stabilization effect. *Composites Part B: Engineering*, **2019**, *162*: 11–20.
- [24] Mousavi-Fakhrabadi S H, Ahmadi S, Arabi H. Mixing of hindered amine-grafted polyolefin elastomers with LDPE to enhance its long-term weathering and photo-stability. *Polymer Degradation and Stability*, **2022**, *198*: 109882.
- [25] Wang B, Tai Q, Nie S, et al. Electron beam irradiation cross linking of halogen-free flame-retardant ethylene vinyl acetate (EVA) copolymer by silica gel microencapsulated ammonium polyphosphate and char-forming agent. *Industrial & Engineering Chemistry Research*, **2011**, *50*: 5596–5605.
- [26] Jia P, Yu X, Lu J, et al. The Re<sub>2</sub>Sn<sub>2</sub>O<sub>7</sub> (Re = Nd, Sm, Gd) on the enhancement of fire safety and physical performance of Polyolefin/IFR cable materials. *Journal of Colloid and Interface Science*, **2022**, *608*: 1652–1661.
- [27] Xiao F, Fontaine G, Bourbigot S. Improvement of flame retardancy and antidripping properties of intumescent polybutylene succinate combining piperazine pyrophosphate and zinc borate. *ACS Applied Polymer Materials*, **2022**, *4*: 1911–1921.
- [28] Liu L, Zhu M, Shi Y, et al. Functionalizing MXene towards highly stretchable, ultratough, fatigue- and fire-resistant polymer nanocomposites. *Chemical Engineering Journal*, **2021**, *424*: 130338.
- [29] Yu F, Jia P, Song L, Hu Y, Wang B, Wu R. Multifunctional fabrics based on copper sulfide with excellent electromagnetic interference shielding performance for medical electronics and physical therapy. *Chemical Engineering Journal*, **2023**, *472*: 145091.
- [30] Jiang X, Chu F, Liu W, et al. An individualized core-shell architecture derived from covalent triazine frameworks: Toward enhancing the flame retardancy, smoke release suppression, and toughness of bismaleimide resin. *ACS Materials Letters*, **2023**, *5*: 630–637.
- [31] Yin Z, Lu J, Hong N, et al. Functionalizing Ti<sub>3</sub>C<sub>2</sub>T<sub>x</sub> for enhancing fire resistance and reducing toxic gases of flexible polyurethane foam composites with reinforced mechanical properties. *Journal of Colloid and Interface Science*, **2022**, *607*: 1300–1312.
- [32] Jia P, Zhu Y, Lu J, et al. Multifunctional fireproof electromagnetic shielding polyurethane films with thermal management performance. *Chemical Engineering Journal*, **2022**, *439*: 135673.
- [33] Wang J, Zhang D, Zhang Y, et al. Construction of multifunctional boron nitride nanosheet towards reducing toxic volatiles (CO and HCN) generation and fire hazard of thermoplastic polyurethane. *Journal of Hazardous Materials*, **2019**, *362*: 482–494.
- [34] Zhang Y, Tian W, Liu L, et al. Eco-friendly flame retardant and electromagnetic interference shielding cotton fabrics with multi-layered coatings. *Chemical Engineering Journal*, **2019**, *372*: 1077–1090.
- [35] Jia P, Yu F, Jin Z, et al. Multifunctional Additive: A novel regulate strategy for improving mechanical property, aging life and fire safety of EVA composites. *Chemical Engineering Journal*, **2023**, *473*: 145283.
- [36] Chen H R, Meng W M, Wang R Y, et al. Engineering highly graphitic carbon quantum dots by catalytic dehydrogenation and carbonization of Ti<sub>3</sub>C<sub>2</sub>T<sub>x</sub>-MXene wrapped polystyrene spheres. *Carbon*, **2022**, *190*: 319–328.
- [37] Wang N N, Wang H, Wang Y Y, et al. Robust, lightweight, hydrophobic, and fire-retarded polyimide/MXene aerogels for effective oil/water separation. *ACS Applied Materials & Interfaces*, **2019**, *11*: 40512–40523.
- [38] Yin Z, Wang B, Tang Q, et al. Inspired by placoid scale to fabricate MXene derivative biomimetic structure on the improvement of interfacial compatibility, mechanical property, and fire safety of epoxy nanocomposites. *Chemical Engineering Journal*, **2022**, *431*: 133489.
- [39] He W, Song P, Yu B, et al. Flame retardant polymeric nanocomposites through the combination of nanomaterials and conventional flame retardants. *Progress in Materials Science*, **2020**, *114*: 100687.